Environmental Research 199 (2021) 111280

Contents lists available at ScienceDirect

Environmental Research

journal homepage: www.elsevier.com/locate/envres

Improvement in air quality and its impact on land surface temperature in major urban areas across India during the first lockdown of the pandemic

Bikash Ranjan Parida [a,*,1], Somnath Bar [a,1], Gareth Roberts [c], Shyama Prasad Mandal [a], Arvind Chandra Pandey [a], Manoj Kumar [b], Jadunandan Dash [c]

[a] Department of Geoinformatics, School of Natural Resource Management, Central University of Jharkhand, Ranchi, 835222, India
[b] Department of Environmental Sciences, School of Natural Resource Management, Central University of Jharkhand, Ranchi, 835222, India
[c] Geography and Environmental Science, University of Southampton, Highfield, Southampton, SO17 1BJ, United Kingdom

ARTICLE INFO

Keywords:
Atmospheric pollutants
AOD
LST
Net radiative flux
Water vapor

ABSTRACT

The SARS CoV-2 (COVID-19) pandemic and the enforced lockdown have reduced the use of surface and air transportation. This study investigates the impact of the lockdown restrictions in India on atmospheric composition, using Sentinel–5Ps retrievals of tropospheric NO_2 concentration and ground-station measurements of NO_2 and $PM_{2.5}$ between March–May in 2019 and 2020. Detailed analysis of the changes to atmospheric composition are carried out over six major urban areas (i.e. Delhi, Mumbai, Kolkata, Chennai, Bangalore, and Hyderabad) by comparing Moderate Resolution Imaging Spectroradiometer (MODIS) Aerosol Optical Depth (AOD) and land surface temperature (LST) measurements in the lockdown year 2020 and pre-lockdown (2015–2019). Satellite-based data showed that NO_2 concentration reduced by 18% (Kolkata), 29% (Hyderabad), 32–34% (Chennai, Mumbai, and Bangalore), and 43% (Delhi). Surface-based concentrations of NO_2, $PM_{2.5}$, and AOD also substantially dropped by 32–74%, 10–42%, and 8–34%, respectively over these major cities during the lockdown period and co-located with the intensity of anthropogenic activity. Only a smaller fraction of the reduction of pollutants was associated with meteorological variability. A substantial negative anomaly was found for LST both in the day (−0.16 °C to −1 °C) and night (−0.63 °C to −2.1 °C) across select all cities, which was also consistent with air temperature measurements. The decreases in LST could be associated with a reduction in pollutants, greenhouse gases and water vapor content. Improvement in air quality with lower urban temperatures due to lockdown may be a temporary effect, but it provides a crucial connection among human activities, air pollution, aerosols, radiative flux, and temperature. The lockdown for a shorter-period showed a significant improvement in environmental quality and provides a strong evidence base for larger scale policy implementation to improve air quality.

1. Introduction

The COVID-19 outbreak is believed to have initially emerged during December 2019 in Wuhan, China (WHO, 2020). Since this time, the pandemic has affected over 196 countries (Wang et al., 2020) with more than 107.9 million COVID-19 cases and 2.3 million deaths (~2.1% mortality rate) worldwide as of February 12, 2021 (JHU, 2021). The WHO declared COVID-19 to be a global public health emergency on January 30, 2020, which follows a number of other health emergencies, including Zika (2016), H1N1 (2009), Polio (2014), and Ebola (2014, 2019). One of the major causes for the rapid spread of the Coronavirus is the ease and widespread use of local, regional and global travel (Munster et al., 2020). As a result, countries around the world implemented travel bans and enforced 'lockdowns' to restrict the population movement in order to reduce the spread of the virus. The enforced lockdowns resulted in a rapid decrease in economic activity due to workplace restrictions, which affected industrial production, non-essential business, transport systems, education establishments, offices, and citizen mobility. Consequently, the use of surface and air transportation reduced globally by 50% and 75%, respectively against the 2019 average (IEA, 2020). The dates at which lockdowns were implemented differed between countries, but most occurred in March (2020) except Hubei, China

* Corresponding author.
E-mail addresses: bikashrp@gmail.com, bikash.parida@cuj.ac.in (B.R. Parida).
[1] These authors contributed equally to this work.

https://doi.org/10.1016/j.envres.2021.111280
Received 24 September 2020; Received in revised form 12 February 2021; Accepted 30 April 2021
Available online 21 May 2021

(January 2020), with the containment measures being eased from the 11th May 2020 in Europe and June 2020 in India, Brazil and USA.

Nitrogen dioxide (NO_2) is a major air pollutant emitted from fossil fuel combustion, power plants, vehicular emissions, biomass burning, and lighting (Beirle et al., 2003; Dentener et al., 2006). Over the years, proliferation in urbanization, industrial activity, and transport emissions has caused increasing emissions of NO_2 leading to a reduction in ambient air quality (Sun et al., 2018; Zheng and Wu, 2019). Globally, it is estimated that NO_x pollution has resulted in nearly 0.1 million deaths (Anenberg et al., 2017), about 4 million asthma cases annually (Achakulwisut et al., 2019) and increased cardiovascular mortality rates and respiratory infections (Chauhan et al., 2003; Chen et al., 2012). Particulate matter (PM) less than 2.5 μg (termed $PM_{2.5}$) is also a major constituent of air pollution and is produced from volcanic activity, dust emissions, and the combustion of fossil fuels and organic matter. The global population-weighted $PM_{2.5}$ has increased by 11.2% from 39.7 (1990) to 44.2 $\mu g/m^3$ in 2015 with India and China having the poorest air quality with population-weighted mean $PM_{2.5}$ concentrations of 74.3 and 58.4 $\mu g/m^3$, respectively in 2015 (Cohen et al., 2017); far exceeding the WHO (2005) recommended daily (25 $\mu g/m^3$) and annual (10 $\mu g/m^3$) average exposure guidelines (Pant et al., 2019; WHO, 2005). Anthropogenic emissions from residential, industrial, and transport sectors are the prevailing source of $PM_{2.5}$ in South Asia and daily concentrations are increasing over time (Crippa et al., 2018). Fine particulate matter causes respiratory and cardiovascular disease, and outdoor air pollution is estimated to have resulted in nearly 4.2 million deaths globally on an annual basis (WHO, 2016; Xing et al., 2016). In India alone, about 16, 000 premature deaths occur annually due to exposure to poor air quality due to $PM_{2.5}$ emissions (Balakrishnan et al., 2019).

The pandemic has resulted in most governments implementing rigorous containment measures, which reduced transport and manufacturing activity. This resulted in a significant reduction in atmospheric pollutants such as CO_2, CO, NO_2, SO_2, PM, and aerosols levels in many industrial countries (Kanniah et al., 2020; Lal et al., 2020; Le et al., 2020; Ranjan et al., 2020; Sharma et al., 2020). For example, CO_2 emissions and energy consumption patterns demonstrated a 17% decrease between January and April (2020) as compared to the same period in 2019, wherein about half of CO_2 emissions were related to surface transport (Le et al., 2020). It has also been reported that global CO_2 emissions decreased by 5.8% in the first quarter (Q1) of 2020 compared to 2019 levels with the largest decreases in emissions due to those from industry (Liu et al., 2020; Safarian et al., 2020). A 1.8% reduction in atmospheric CO_2 concentration was found using in-situ surface monitoring station data in the Peninsular Malaysia during the lockdown in Q1 of 2020 compared to that of the mean of the same Q1 in 2017–18 (Yang et al., 2016). These changes are mainly attributed to the shutdown of industry, surface transport, and aviation due to the pandemic restrictions. CO_2 flux data from several urban sites has revealed that CO_2 flux has decreased by 8% in an area of Berlin dominated by vegetated cover (Germany) and 75% in the centre of Heraklion, Greece (Papale, 2020). The atmospheric CO_2 concentration across several sites in Kolkata and nearby Islands Sundarbans, India, also decreased substantially (18–39%) during the lockdown (Parida et al., 2020). However, changes in CO_2 concentration were not detected at the global monitoring station in Mauna Loa Observatory (MLO) (Parida et al., 2020).

A decline in NO_2 concentrations of up to 30% has been detected in cities in China, India, Malaysia, Europe, and the USA (Abdullah et al., 2020; Dutheil et al., 2020; Muhammad et al., 2020; Shrestha et al., 2020; Tobías et al., 2020; Wang, 2020; Zhang et al., 2020). In central China, NO_2 concentrations decreased by 61% (Xu et al., 2020) whilst in eastern China, reductions of 30% occurred due to the lower usage of coal and oil (Filonchyk et al., 2020). The average of 336 cities across China showed a reduction of 14% and 16% of $PM_{2.5}$ and NO_2, respectively (Chen et al., 2020). Similarly large reductions in NO_2 and $PM_{2.5}$ concentrations (53% and 35–39% respectively) have been identified in urban areas in India (Chauhan and Singh, 2020; Mahato et al., 2020; Navinya et al., 2020). In Brazil and Spain, large reductions in NO_2 and PM_{10} concentrations have also been found and are attributed to the reduction in vehicular emissions (Dantas et al., 2020; Siciliano et al., 2020; Tobías et al., 2020).

Aerosol concentrations have also reduced by 40–60% during lockdowns over several cities in India and South Asia (Gautam, 2020; Kanniah et al., 2020; Ranjan et al., 2020) and aerosols impact the net radiation at the top and bottom of the atmosphere through their direct and indirect effects on solar radiation (Lin et al., 2015). The direct impacts (i.e. scattering and absorbing solar radiation) generally reduces surface temperature over urban/industrial regions by reducing surface insolation (Jin et al, 2005, 2010, 2005; Kaufman and Koren, 2006). However, the indirect effect (i.e. aerosol-cloud-interaction) is more complex, uncertain, and highly variable which has implications on the surface energy balance (Rosenfeld, 2000; Tibbetts, 2015). The aerosol–temperature relationship is predominantly negative in India and China across except during summer where higher Aerosol Optical Depth (AOD) concentrations result in lower temperatures (Li et al., 2009; Roy, 2008).

Numerous studies have found correspondence between PM concentration and land surface temperature (LST, Kim, 2019) and the urban heat island (UHI) (Jin et al., 2010; Pandey et al., 2014). Changes in PM concentration during the lockdown provide the opportunity to investigate its impact on the LST over key urban areas of India. This study aims to investigate the influence of anthropogenic activity on LST during the pandemic when anthropogenic activities and their associated emissions were curtailed. The overarching objectives of this study are to: (1) quantify the changes in pollutant and aerosol (NO_2, $PM_{2.5}$ and AOD) levels across six major urban areas in India as a result of the enforced pandemic lockdown and to perceive implications of reduced emissions on surface temperature, and (2) investigate whether changes in atmospheric pollutants, water vapor, and net radiative flux during the pandemic have impacted the LST and UHI. To do so, measurements of the tropospheric NO_2 and surface measured $PM_{2.5}$ concentration made between March and May 2020 will be compared with those obtained over the same months in 2019 over the six most populated cities of India.

2. Data and methods

Satellite-derived measurements of NO_2, AOD, Absorption Aerosol Optical Depth (AAOD), net radiative flux, and LST and ground measurements of NO_2, $PM_{2.5}$, and air temperature (AT) are used to provide a comprehensive estimate of the impact of lockdown on air pollution and urban temperature over six major populous cities of India. The data are described in detail in the following sections.

2.1. Sentinel–5Ps TROPOMI data

The Copernicus satellite Sentinel–5P, launched in October 2017, carries onboard the Tropospheric Monitoring Instrument (TROPOMI) instrument, which acquires daily observations at a spatial resolution of 3.5 × 7 km. The TROPOMI instrument has four separate spectrometers, which cover spectral ranges in the ultraviolet and near-infrared (0.27–0.5 μm and 0.675–0.775 μm) and the shortwave infra-red (2.305–2.385 μm) (Griffin et al., 2019). These instruments make retrievals of a number of gases, such as ozone (O_3), NO_2, and sulphur dioxide (SO_2) (Veefkind et al., 2012).

The NO_2 retrieval algorithm was initially developed by using the ultraviolet and near-infrared bands (0.27–0.5 μm), which was adopted from Ozone Monitoring Instrument (OMI)-based NO_2 retrieval (Boersma et al., 2004; Zara et al., 2018). The retrieval is based on the DOAS (differential optical absorption spectroscopy) spectral-fitting technique (Cede et al., 2006). The NO_2 column density retrievals characterize the vertically integrated number of NO_2 molecules per unit area between the surface and the tropopause with typical column density concentrations ranging between 10 and 200 $\mu mol/m^2$ worldwide (Griffin et al., 2019).

The TROPOMI NO_2 product has been widely tested and validated using *in-situ* measurements and demonstrated a high correlation with a low negative bias (Griffin et al., 2019; Ialongo et al., 2020; McLinden et al., 2012). In this study, tropospheric NO_2 column density product for January–May 2019 and 2020 were obtained from the Google Earth Engine (GEE) Data Repository using API code developed in GEE (Gorelick et al., 2017).

2.2. Land surface temperature (LST) (MOD11A1)

The MODIS LST product (MOD11A1) (Wan, 2008) collection 6 provides day and night LST estimates at 1-km spatial resolution covering an area 1200 by 1200 km. LST estimates are derived using the split-window algorithm (Wan and Dozier, 1996) applied to atmospherically corrected longwave infrared channels (bands 31 and 32). Validation of the MODIS LST product indicates the mean LST error is within ±0.6 K when assessed using in-situ observations at ten validation sites and within ±1 K in 39 of 47 sites (Wan, 2014). In this study, day and night MODIS Terra LST data were acquired from the GEE Repository between March and May over the past six years (2015–2020).

2.3. Aerosol Optical Depth (AOD) (MCD19A2) and AAOD (OMI-derived)

The MODIS Aerosol Optical Depth product (MCD19A2) collection 6 provides AOD estimates at 1-km spatial resolution covering an area 1200 by 1200 km. This is a combined Level–2 gridded daily product of Terra & Aqua with Multi-angle Implementation of Atmospheric Correction (MAIAC, Lyapustin et al., 2012). The MAIAC algorithm-based AOD has been found to have higher accuracy than the MODIS dark target and deep blue algorithms over dark surfaces and smoke plumes (Mhawish et al., 2019). The MAIAC was obtained from the GEE repository between March and May over the past six years (2015–2020). The daily AAOD (OMAERUVd v003 Level-3) at 550 nm is available at a grid resolution of $1^\circ \times 1^\circ$ which was retrieved from OMI using the OMAERUV algorithm (Torres et al., 2018). This dataset is acquired over the past six years (2015–2020) to analyze its association with temperature.

2.4. Net radiative flux at TOA (around 20-km altitude) and surface

The net radiative flux both at TOA and Surface (Level–3b) data were obtained for the period 2015–19 (March–May) from the Clouds and the Earth's Radiant Energy System (CERES) Energy Balanced and Filled (EBAF) data product (https://ceres.larc.nasa.gov/data). This dataset is available at a spatial resolution of $1^\circ \times 1^\circ$ and a monthly temporal resolution. The net flux at TOA and Surface for all-sky and clear-sky conditions were used in this analysis. The TOA net flux is calculated as the difference between the total downwelling incoming solar radiation, and the upwelling reflected shortwave and emitted longwave radiation at the TOA (Loeb et al., 2018). The EBAF net flux data for 2020 is not available, and instead, the Fast Longwave and Shortwave Radiative Flux product (FLASHFlux; Kratz et al., 2014) is used, which merges CERES and MODIS short and longwave flux measurements. In this study, the net radiative flux at TOA and surface over the period April–May 2020 were employed to analyze its association with temperature.

2.5. Atmospheric column water vapor content and aerosol sources

The Modern-Era Retrospective analysis for Research and Applications (MERRA-2) provides a global dataset on atmospheric water vapor content. The total precipitable water vapor data has been retrieved from the Giovanni platform (https://giovanni.gsfc.nasa.gov/giovanni). The aerosol type sources such as black carbon (BC), organic carbon (OC), mineral dust, sea salt, and SO_2 were acquired from MERRA-2. These data are available at a daily temporal resolution and $0.5^\circ \times 0.625^\circ$ spatial resolution. The water vapor content is also retrieved from the NCEP/NCAR Reanalysis (spatial resolution $2.5^\circ \times 2.5^\circ$) and is available in the GEE Repository.

2.6. Meteorological parameters from ERA-5

Meteorological variables, namely relative humidity, precipitation, wind speed and direction, and boundary-layer height (BLH), are from the European Centre for Medium-Range Weather Forecasts (ECMWF) global atmospheric reanalysis (ERA5) dataset. All meteorological variables are at daily temporal resolution, except the BLH, which is at monthly temporal resolution and $0.5^\circ \times 0.5^\circ$ spatial resolution (precipitation at $0.25^\circ \times 0.25^\circ$ resolution). These data are available in Copernicus platform (https://climate.copernicus.eu/climate-reanalysis). The wind and relative humidity datasets are 1000 hPa above the surface.

2.7. In-situ air temperature, NO_2 and $PM_{2.5}$ data from ground-based stations

The station-based air temperature (AT) measurements were collected at six locations in India for the months March to May between 2015 and 2020. The sites are Safdarjung Airport (New Delhi 28.59 °N, 77.21 °E), Chhatrapati Shivaji International Airport (Mumbai 19.09 °N, 72.86 °E), Kolkata (Behala Airport 22.54 °N, 88.34 °E), Chennai (KK Nagar AWS Station 13.04 °N, 80.19 °E), Bangalore (Kasturi Nagar Station 12.97 °N, 77.6 °E), and Hyderabad (Rajiv Gandhi Int. Airport Station 17.25 °N, 78.43 °E). The AT data, accessed via the Weather Underground site, comprise of the average daily maximum and mean day-time air temperature (Tmax, Tmean) and minimum night-time air temperature (Tmin) (Weather Underground, 2020). Daily average NO_2 and $PM_{2.5}$ data were acquired from surface stations located in six cities in India as part of the Citizen Weather Observer Program (CWOP, 2020). Daily data, which were averaged to weekly temporal resolution, were obtained between March–May in 2019 and 2020 for comparison to coincident satellite-derived measures.

2.8. Gridded global human modification (gHM) and population density

Global human modification (gHM, Kennedy et al., 2019) and population density (SEDAC, 2020) ~ 1 km data were used to investigate the relationship between atmospheric pollution and the intensity of anthropogenic activity. The gHM is a cumulative measure of human land modification related to human settlement, agriculture, population density, built-up, transport and utilities (i.e. road, railways, and power lines), night-time lights, and mining activities. The HM ranges from 0 (no modification) to 1 (fully modified). These datasets have been validated against high-resolution aerial and satellite imagery with good agreement ($r = 0.78$) found between HM and the validation dataset at national to global scales (Chu et al., 2020; Theobald et al., 2020).

2.9. Methods

The mean NO_2 concentration ($\mu mol/m^2$) within a 20-km radius of each urban area (e.g. New Delhi, Mumbai, Kolkata, Chennai, Bangalore, and Hyderabad) was calculated using the available daily NO_2 retrievals over the period March to May (i.e. the lockdown duration) for 2019 and 2020. From these data, the standardized simple anomaly was calculated to characterize the percentage difference in tropospheric NO_2 concentration between 2019 and 2020. The standardized anomaly was also calculated for the MODIS LST and AOD, AAOD, CERES net radiative flux, and surface air temperature estimates using the demi-decadal mean over the period March–May between 2015 and 2019. The percentage difference in meteorological parameters (RH, Wind speed, BLH, precipitation) and atmospheric water vapor content was calculated between 2020 and the mean of 2015–2019 to assess the relationship

between metrological conditions and air pollutants.

3. Results

3.1. Variation in NO_2 and $PM_{2.5}$ across six urban areas

In India, the lockdown was implemented on 24th March 2020 and during this period, all industry, institutions, and transportation ceased. The satellite-derived mean tropospheric NO_2 reveals much lower NO_2 concentrations in 2020 compared to the same period in 2019 across all six cities. Over Delhi and Mumbai, the mean NO_2 concentration ranged between 200 and 300 μmol/m^2 in 2019 as opposed to between 100 and 200 μmol/m^2 in 2020. In the remaining cities, the mean NO_2 concentration was on average 18–34 μmol/m^2 lower in 2020 compared to 2019. Fig. 1 presents the standardized anomaly showing the percentage difference in NO_2 between March and May in 2019 and 2020 for each urban area. It is clear that all cities of India have seen a large reduction in NO_2 concentration with average city-wide reductions of between 18 and 43% (Table 1) and an overall average decrease in NO_2 of 31.5%. Kolkata deviates from the other cities with a much lower reduction in NO_2 (18.1%). The areas with the greatest reduction in NO_2 concentration are those with the highest gHM and population density (Fig. S1). The spatial distribution of the average tropospheric NO_2 concentration showed the greatest reduction in the urban centres of Delhi, Mumbai and Chennai which typically have higher population densities and higher intensity of human activity (i.e. human settlement, build-up area, agriculture, transport, and industrial, among others) as indicated by gHM (Fig. S1). The gHM dataset indicates that the mean gHM exceeded 0.75 in all six cities and higher mean population density witnessed in Mumbai (34,998 person/sq.km), Kolkata (28,670 person/sq.km), and Delhi (21,484 person/sq.km) followed by Chennai (19,822 person/sq.km), Hyderabad (14,264 person/sq.km), and Bangalore (9509 person/sq.km) (Fig. S2).

The ground-station based weekly average NO_2 and $PM_{2.5}$ concentration for 2019 and 2020 is presented in Figs. S3–S4 across each cities. The temporal trends of the weekly NO_2 and $PM_{2.5}$ data highlight the decline in concentration across these major urban areas and is particularly evident in Delhi. The concentrations in March 2019 and 2020 are typically in closer agreement as the lockdown measures were not implemented until the end of March. After this time, greater differences are apparent in concentrations between 2019 and 2020, although Hyderabad departs from this trend from mid of May as the lockdown was de-escalated whilst the $PM_{2.5}$ concentration was higher in 2019. Fig. 2 summarises the percentage anomaly in NO_2 and $PM_{2.5}$ and reveals the NO_2 concentration reduced by between 32% (Hyderabad) and 74% (Delhi) (Table 1) whilst $PM_{2.5}$ concentrations displayed lower reductions of between 9% (Mumbai) and 42% (Bangalore). The daily surface measured NO_2 and satellite retrievals of NO_2 (Table 1) indicate Delhi records the greatest average reduction but that the anomaly percentage is higher from the surface stations than the satellite retrievals where the average reduction is 55.6% and 31.5% respectively. This is due to the surface stations being located at airports where the reduction in transportation is likely to be more profound impact on NO_2 concentration than that found in city centres where some transportation was still operational. The $PM_{2.5}$ displays lower reductions than the NO_2, particularly in Mumbai and Kolkata, as emissions due to sea salt, dust, and cooking fuel are likely to remain to various degrees.

Table 1
Average anomaly and standard errors (±se) in NO_2 and $PM_{2.5}$ concentration between 2020 and 2019 using observations during the lockdown period (24th March to 18th May).

Ground stations	Anomaly (%) (satellite-derived)	Anomaly (%) (surface station measurement)	
	NO_2	NO_2	$PM_{2.5}$
Delhi	−43.06 (±0.22)	−74.05 (±1.90)	−26.96 (±3.06)
Mumbai	−33.39 (±0.29)	−45.60 (±3.56)	−9.08 (±3.11)
Kolkata	−18.19 (±0.52)	−57.77 (±2.64)	−23.86 (±4.23)
Chennai	−31.77 (±0.13)	−61.19 (±3.30)	−37.08 (±3.38)
Bangalore	−33.88 (±0.14)	−63.01 (±1.59)	−41.71 (±2.51)
Hyderabad	−29.10 (±0.11)	−32.00 (±4.39)	−19.00 (±2.89)

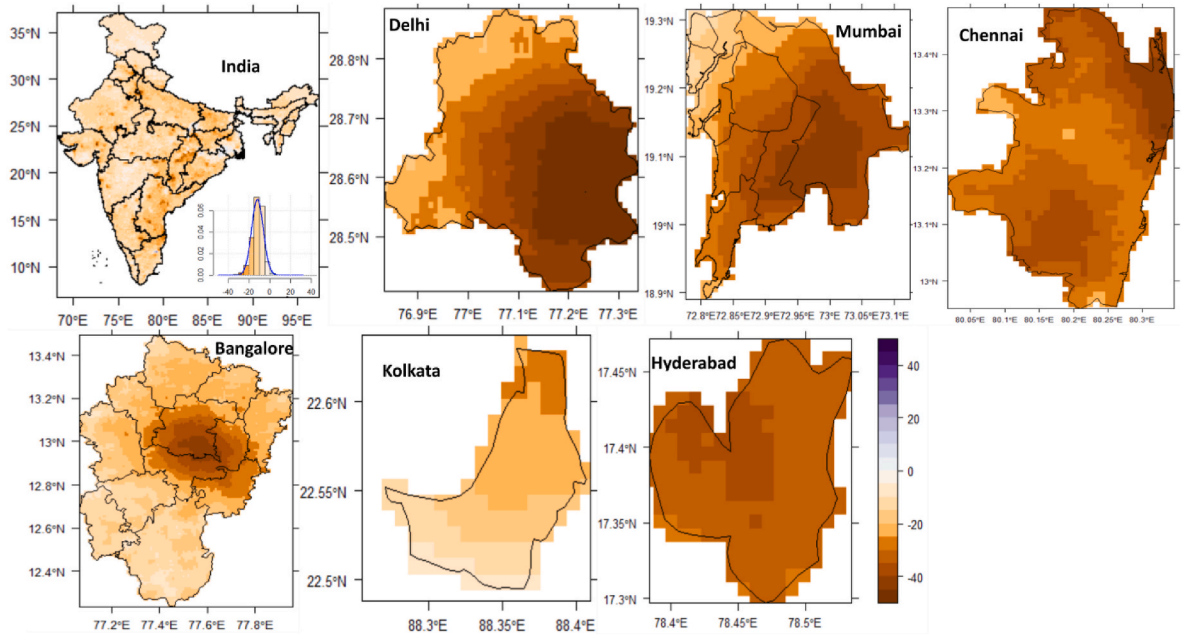

Fig. 1. Present anomlay of mean tropospheric NO_2 concentration during effective lockdown period (i.e. 24th March–18th May) in 2020 across India and in six large cities.

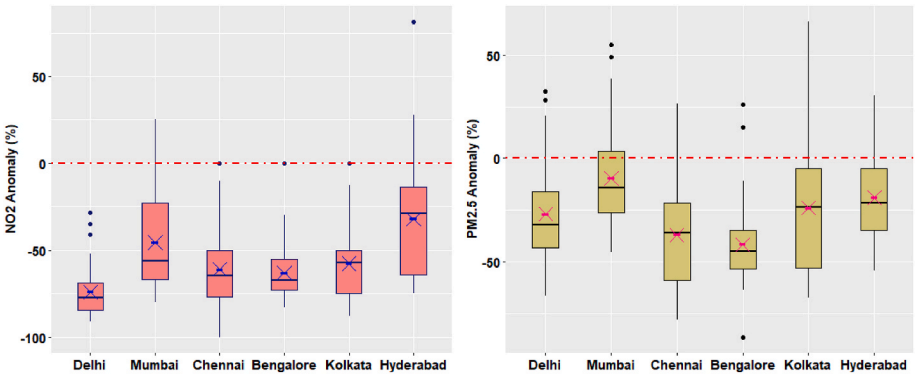

Fig. 2. Box plots showing the percentage anomalies in NO_2 and $PM_{2.5}$ concentration measured from surface stations in six cities. The bars show the mean and the cross the median values derived from the average daily concentrations.

3.2. *Variation in NO_2 and $PM_{2.5}$ in relation to meteorological conditions*

Fig. 3 shows meteorological variability in 2020 than that of the average condition over 2015–19 as it might be an additional contributing factor in reducing atmospheric pollutants. A widespread increase in relative humidity by 15–25% was found across India during the pre-monsoon season (March–May), enabling aerosol formation (Fig. 3A). The wind speed declined by 10–25% and winds mostly originated from the Arabian Sea (Fig. 3B), which helps to transport mineral dust from the Thar desert towards the interior landmass. This might contribute to haze formation over parts of Central India as evidenced by the positive AOD anomalies (Fig. 4), but decreased wind speed does not facilitate the dispersion of pollutants (Goldberg et al., 2020). The PBL height is 20–40% lower (Fig. 3C), indicating the formation of a stable boundary layer and stationary air, and these conditions are suitable for increasing pollutants (Le et al., 2020). However, some regions also display a

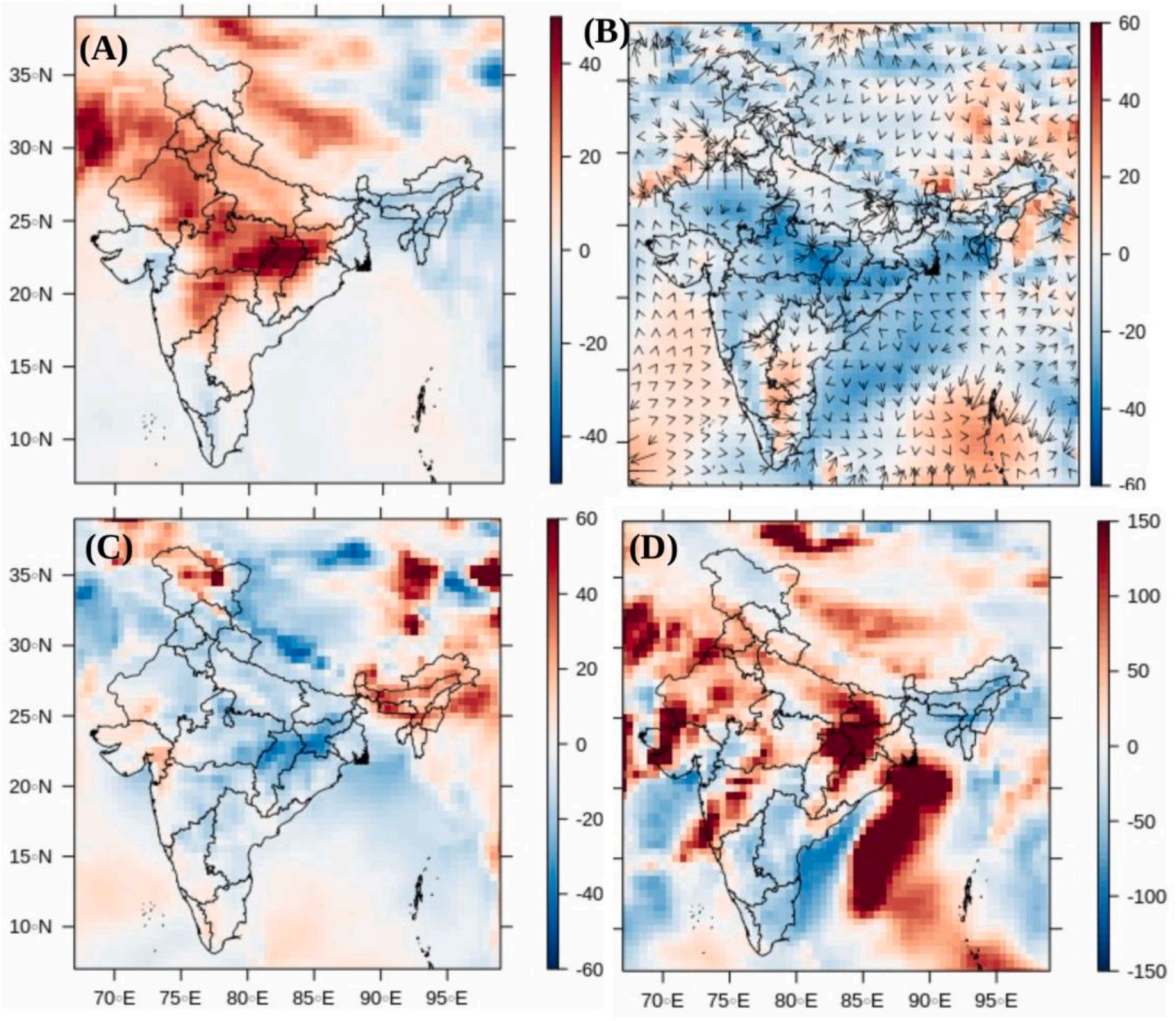

Fig. 3. Percentage change in ERA-5 meteorological variables in 2020 relative to the average over the period 2015–19 (i.e. March–May). (A) relative humidity, (B) wind speed at 1000 hPa pressure level, (C) boundary-layer height, and (D) precipitation. In B) the overlaid wind direction is that from 2020.

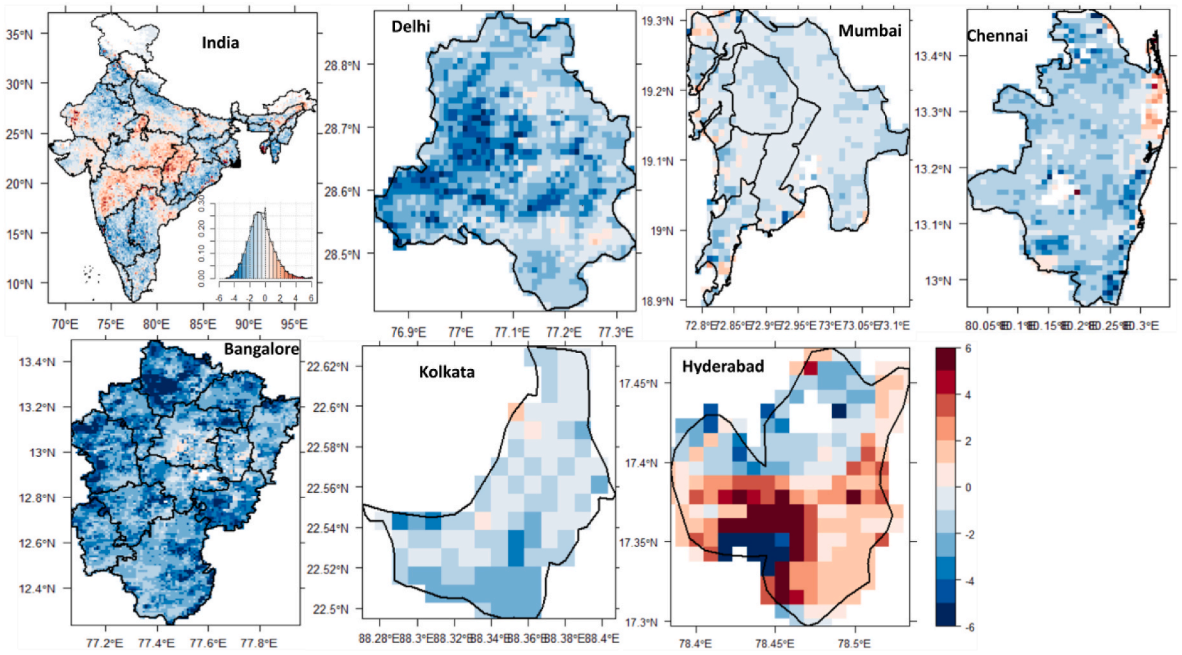

Fig. 4. Present standardized AOD anomaly during 24th March–18th May across India and over six cities against the demi-decadal mean over the same time period for the years 2015–19.

moderate increase in PBL height. Precipitation shows a mostly positive increases in northern and west-central regions and a decreasing pattern over southern India (Fig. 3D). Combined the anomalies in meteorological conditions that can influence the vertical distribution of pollutants are not believed to play a significant role in the observed reduction of pollutant concentration across India.

3.3. AOD and temperature variation (March–May)

It is evident that the changes in working and travel patterns has resulted in a large reduction of NO_2 and $PM_{2.5}$ concentrations, particularly over densely populated areas. Fig. 4 shows the standardized AOD anomaly across India as well as for each urban area, which indicates most areas saw a reduction in optical depth. An exception is Hyderabad located in central India, where increases and decreases in AOD are evident which may result from local supply of mineral dust aerosols from the north western arid region and emissions from industrial sources. Meteorological conditions may also play a role although it is less clear as regions of positive AOD (e.g. Maharashtra state) can coincide with positive precipitation anomaly (Fig. 3d). The AOD anomaly displays lower spatial coherence than that found with NO_2 (Fig. 1) partly due to the wider range of PM emissions sources, which sees some areas in each city showing an increase in AOD. The mean AOD anomaly for Delhi, Mumbai, Kolkata, Chennai, Bangalore, and Hyderabad was −1.78, −0.93, −2.69, −3.39, and −1.75, and −0.2 respectively (Table 2).

It was evident that there has been a reduction in atmospheric NO_2, $PM_{2.5}$, and AOD as measured by both satellite retrievals and surface station measurements during the pandemic. We investigate whether these changes in atmospheric composition impact the land surface and air temperature in each city using satellite and ground-station data.

The MODIS LST anomaly in 2020 (both day and night-time) against long-term averages (2015–2019) for India and each city is presented in Figs. 5–7. Widespread negative LST anomalies are found across India with 81.6% and 79.6% of the land surface having seeing reductions in night and day LST respectively. Positive LST anomalies, which have been associated with a reduction in aerosol concentration and atmospheric scattering during the lockdown (Westervelt et al., 2020; Yang et al., 2016), were found in Southern peninsular and Northeast India (Fig. 5). This region is largely composed of negative AOD anomalies (Fig. 4) although many areas of India have both negative AOD and LST anomalies. Negative night-time LST anomalies are found across four cities (Delhi, Chennai, Hyderabad, and Bangalore) whilst Kolkata and Mumbai display positive anomalies (Table 2). The positive anomalies in Mumbai and Kolkata are believed to be associated with the sea breeze effect contributing to an increase in night-time temperature (Fig. 6, (Pal et al., 2020). The relationship between the daytime LST (Fig. 7) and AOD (Fig. 3) anomalies is somewhat mixed with only Delhi showing a consistent decrease in both which may be linked to changes in residual burning practices in Punjab as well as reduced frequency of forest fire during the pre-monsoon season (Gupta et al., 2020). Fig. S5a shows the anomalies in Organic (OC) and Black Carbon (BC), emitted through fossil fuel combustion and biomass burning, which shows a large negative anomaly over the Punjab where crop residue burning is widespread with the smoke being transported over Delhi (Liu et al., 2018). The strong radiative absorption characteristics of BC can to lead to reductions in daytime LST (Qian et al., 2006). The variable

Table 2
Mean AOD and temperature anomalies (24th March–18th May) in 2020 against demi-decadal observation (2015–2019) over six cities in India.

City		LST anomalies °C (±SE)		AT anomalies °C	
	AOD anomalies	Mean Night LST anomaly	Mean Day LST anomaly	Tmin (Night)	Tmax (Day)
Delhi	−1.78 (±0.011)	−2.10 (±0.016)	−1.04 (±0.005)	−0.82	−1.04
Mumbai	−0.93 (±0.015)	1.43 (±0.023)	0.84 (±0.02)	0.36	0.08
Kolkata	−2.69 (±0.056)	1.25 (±0.02)	2.5 (±0.03)	−0.77	−0.75
Bangalore	−3.39 (±0.016)	−0.63 (±0.004)	−0.16 (±0.004)	−0.58	−0.80
Chennai	−1.75 (±0.02)	−1.75 (±0.019)	−0.93 (±0.016)	−0.83	−0.84
Hyderabad	−0.2 (±0.03)	−0.5 (±0.01)	−0.21 (±0.01)	0.48	−1.48

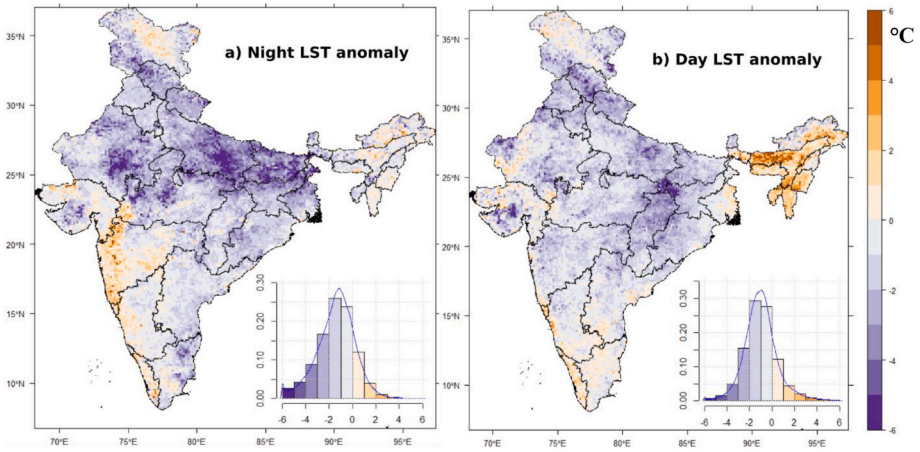

Fig. 5. Standardized (a) night-time MODIS LST and (b) day-time MODIS LST anomalies (°C) during 2020 (24th March–18th May) against the demi-decadal mean for the years 2015–19. The histogram showing distribution of positive and negative pixels.

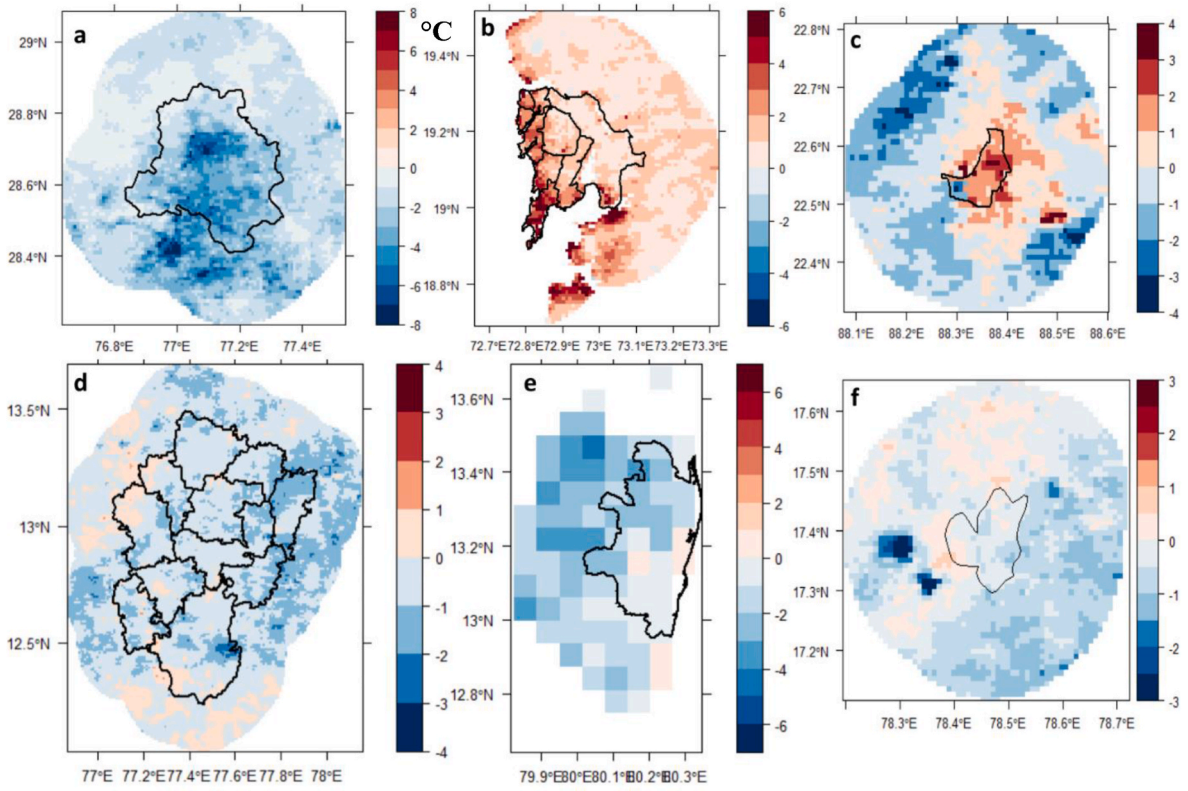

Fig. 6. Standardized night-time LST anomalies (°C) during 2020 (24th March–18th May) over (a) Delhi, (b) Mumbai, (c) Kolkata, (d) Bangalore, (e) Chennai, and (f) Hyderabad city. A 20-km buffer has been applied from the city boundary.

relationship between daytime LST and AOD anomalies may result from variations in the planetary boundary layer (Fig. 3a) and precipitation (Fig. 3d) which increase the variation in aerosol concentration and remove aerosols from the atmosphere respectively.

The ground station-based air temperature (AT) anomalies (Fig. 8) for 2020 (24th March–18th May) was computed both for day-time (Tmax) and night-time temperature (Tmin), against data from the same months but between 2015 and 2019. As found with the MODIS LST anomalies, the AT anomalies are low and largely negative with the exception of Mumbai and Hyderabad. Among the cities, Delhi has the largest combined negative LST and AT anomalies (Table 2) whilst Mumbai has positive day and night AT anomalies which are in line with the MODIS LST anomalies. However, the MODIS LST and in-situ AT anomalies differ in Kolkata where the in-situ mean AT anomaly is negative (−0.75 °C and −0.77 °C for Tmax and Tmin respectively) and the day-time MODIS LST anomaly is positive. Notably in Delhi, there were about 13 wet days out of 56 days, and thus, the wet days have helped accelerate this wide reduction of temperature, which can be seen from the outliers. It can be noted that there were no wet days in Chennai, Bangalore, Hyderabad, and Mumbai in 2020 during 24th March–18th May, mostly due to the dry season in India.

The reduction in suspended particulate matter and other air pollutants in the lower atmosphere may contribute to the reduction in surface and air temperature (Bera et al., 2020) and this is investigated further in the subsequent section through an analysis of the net radiative flux at the surface and TOA.

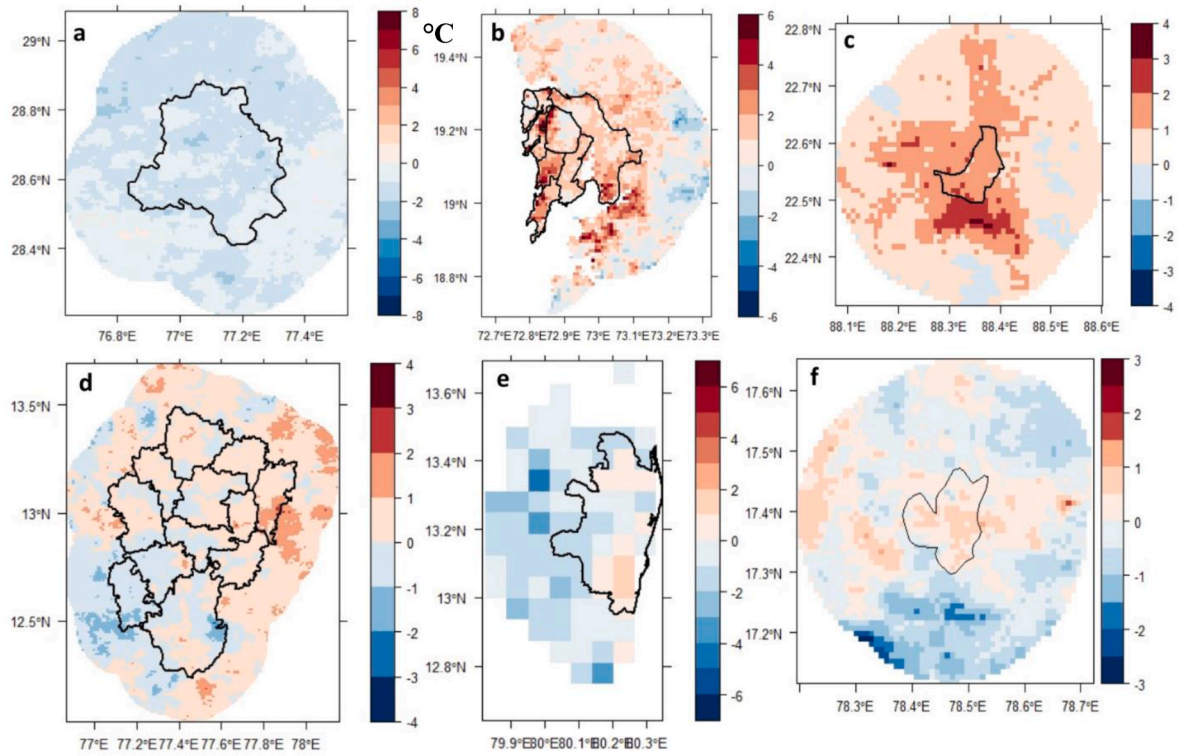

Fig. 7. Standardized day-time LST anomalies (°C) during 2020 (24th March–18th May) over (a) Delhi, (b) Mumbai, (c) Kolkata, (d) Bangalore, (e) Chennai, and (f) Hyderabad city. A 20-km buffer has been applied from the city boundary.

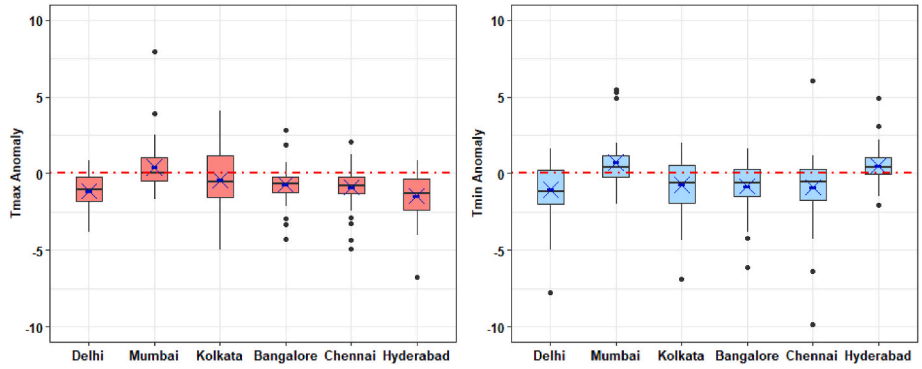

Fig. 8. Ground-station standardized air temperature anomalies (Tmax and Tmin in °C) from daily average measurements in 2020 (24th March–18th May) over each city.

3.4. Top of the atmosphere (TOA) and surface net of net radiation flux anomalies

Anomalies in the average net raditaive flux (i.e. all-sky and clear-sky conditions) at the top of the atmosphere (TOA) and at the surface in 2020 (March–May) is shown in Fig. S6, which are negative over many regions in India. The net raditaive flux at the surface (all-sky) exhibits a negative anomaly between −10.6 W m^{-2} (Kolkata) and −2.8 W m^{-2} (Hyderabad) across all cities except Chennai (0.45 Wm^{-2}) and Bangalore (1.8 Wm^{-2}) (Fig. 9). The net TOA flux (all-sky and clear sky) displayed negative anomalies in all cities but with a lower magnitude than that found at the surface. A decrease in the net radiative flux in Madrid during the lockdown was attributed to reductions in aerosol emissions (Barragan et al., 2020). The average decrease over East Asia was 3.8 W m^{-2} (or 7%) in March 2020 and one-third of the clear-sky anomalies was attributed to emission reductions during the lockdown, and the rest due to natural variability (Ming et al., 2021). Here, a positive anomaly in the net radiative flux is detected at Chennai (0.45 W m^{-2}) and Bangalore (1.8 W m^{-2}), both of which are largely characterised by a reduction in AOD (Fig. 4). It is clear that, whilst there is some indication that reduction in anthropogenic emissions has influenced surface temperature and net radiative flux in these urban areas (Gogoi et al., 2019), other factors such as local climatology, surface heterogeneity and variations in lockdown efficacy also play a role.

3.5. Percent changes in atmospheric total column water vapor

The change in total column water vapor in 2020 relatively to the long-term averages (2015–2019) over India is shown in Fig. S7 which largely shows an increase in water vapor across India for both MERRA-2 and NCEP datasets with the exception of the north-east. Total column water vapor content increases across all five cities by between 0.5 and 19% (MERRA-2) and 4 and 11% (NCEP) with the exception of Chennai (Table S1) which coincides with an increase in relative humidity

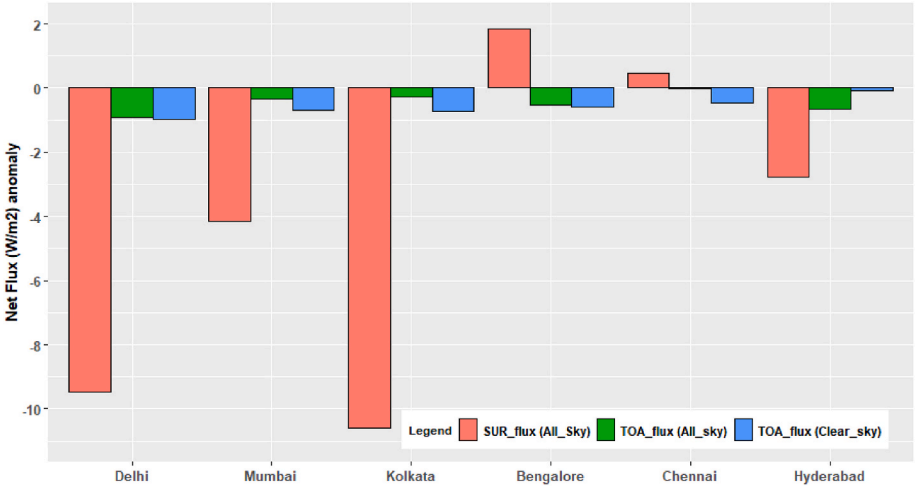

Fig. 9. Present standardized net radiative flux anomalies at top of the atmosphere (TOA) and surface (All-sky and clear-sky condition) during 2020 against the demi-decadal mean 2015–19 (i.e. April–May) for each city.

(Fig. 3a). The decline in net radiative flux might be attributed to an increase in water vapor by increasing the absolute magnitude of the shortwave cloud radiative forcing (CRF) through the lower-tropospheric large-scale air circulation that makes a higher water content in clouds. It is possible that the shortwave CRF effect might be larger than the small changes in the outgoing longwave radiation (OLR) (Barragan et al., 2020). Consequently, it contributed to a decrease in net radiative flux at TOA (Larson and Hartmann, 2003). The shortwave CRF effect seems to be the dominant one, and thus the clouds have induced a decrease in the net downward radiation flux at the TOA.

4. Discussion

The COVID-19 pandemic and nation-wide lockdowns have had a considerable impact on the economy and environment due to the cessation of industrial activities, transportation networks, agricultural practices, non-essential business, and citizen mobility. These activities are sources of atmospheric pollutants and aerosols emissions, largely through fuel combustion. This study assessed the changes in atmospheric pollutants (NO_2 and $PM_{2.5}$) and aerosols (AOD) during the lockdown (2020) relative to the same period in 2019 over six populous cities in India.

The satellite-based analysis demonstrated that tropospheric NO_2 concentrations had reduced by 18% (Kolkata), 29% (Hyderabad), 32–34% (Chennai, Mumbai, Bangalore), and 43% (Delhi). Among these six cities, surface-based NO_2 levels reduced by between 74% (Delhi) and 32% (Hyderabad) whilst $PM_{2.5}$ decreased by 41% (Bangalore) and 9% (Mumbai). In India, several studies have also demonstrated significant reduction in NO_2 emissions across several Indian cities during lockdown (Acharya et al., 2021; Bera et al., 2020; Biswal et al., 2020; Singh et al., 2020). Vadrevu et al. (2020), analysed the air pollution in 41 cities across India and similarly found decreases in tropospheric NO_2 in Delhi (60%), Bangalore (48%), Ahmedabad (46%), Nagpur (46%), Gandhinagar (45%), and Mumbai (43.08%). The effects in coastal cities were lower (~22% NO_2 reduction) which is attributed the influence of the wind and sea breeze (Vadrevu et al., 2020). Numerous studies have also detected decreases in $PM_{2.5}$ concentration of between 19 and 54% in major cities across India during the first lockdown of the pandemic (Chauhan and Singh, 2020; Jain and Sharma, 2020; Kumar et al., 2020; Kumar, 2020; Mahato et al., 2020; Sharma et al., 2020).

Analysis of the MODIS AOD product found that negative anomalies occurred over large parts of India although parts of central India and locations of mining activities exhibited positive AOD anomalies. All cities exhibited negative anomalies (Table 2) with the highest negative standardized anomaly of AOD occurred in Bangalore (−3.4) whilst the lowest was in Mumbai (−0.93), and all cities exhibited negative anomalies (Table 2). The reduction of AOD in 2020 was found to be 20–60%, 10–50%, 25–80%, 30–75%, and 40–80%, in Delhi, Mumbai, Kolkata, Chennai, and Bangalore, respectively. However, in Hyderabad, both increases and decreases of AOD were found of 10–30%. The reduction in the concentrations of atmospheric pollutants and aerosols observed over these cities are comparable with the results from similar studies (e.g. Chauhan and Singh, 2020; Kanniah et al., 2020; Ranjan et al., 2020; Siddiqui et al., 2020). For instance, the AOD level reduced by 6–37% over urban areas in India (Acharya et al., 2021; Ranjan et al., 2020). The anomalies in AOD are more variable than those found with NO_2 partly as a result of the greater range of emissions sources of atmospheric aerosols which is illustrated by the positive AOD anomalies in mining regions in central India (Fig. 3a; Bera et al., 2020). Contributing to the variability in atmospheric composition is meteorological conditions which can reduce atmospheric aerosols through precipitation and transport. Here, only a small fraction of the pollutant reduction is believed to be associated with meteorological conditions which is consistent with the findings of Navinya et al. (2020) who found the shutting down commercial/industrial and transport activities to have a greater impact over several urban areas of India. Analysis of the total column NO_2 over cities in North America found differences of ~15% due to changes in meteorological conditions (Goldberg et al., 2020) whilst changes in NO_2 as a result of the pandemic have varied between 22 and 60% (India, this study) and by between 18 and 40% in cities in China, Western Europe, and North America (Bauwens et al., 2020).

Variation in land surface temperature and ground-based air temperature anomalies revealed a widespread negative anomaly across much of India and over major cities which ranged from–2.1 (Delhi) to −0.63 °C (Bangalore) and –1.04 (Delhi) to −0.16 °C (Bangalore) during the night and day respectively (Table 2). Similar results were found in ground-based air temperature measurements which were also largely negative with the exception Mumbai. Similar reductions in LST during the pandemic have been found in Kolkata (Bera et al., 2020; Sahani et al., 2020) and the Dwarka river basin (West Bengal province, Mandal and Pal et al., 2020) where average Landsat-derived LST decreases of between 0.2 and 5 °C have been reported and which attributed to reduction in atmospheric pollutants and aerosols. In their analysis of Landsat LST over a number of large cities in India during the pandemic, Nanda et al. (2021) also found most exhibited a decreases in LST except Kolkata which saw in increase in surface temperature. Natural processes and anthropogenic activities influence the LST including the local metrological conditions and variations in surface heterogeneity and

condition. However, the decreasing concentration of atmospheric pollutants could modify the surface temperature by attenuating surface solar radiation through scattering and absorption (Yang et al., 2016). Higher particulate matter concentrations have been related to increases in LST (Jin et al., 2010) but can lead to increases and decreases in LST due to increased scattering of shortwave radiation and trapping of longwave radiation respectively (Li et al., 2018; Song et al., 2018). The complex interaction between AOD and LST is illustrated by the largely negative AOD anomalies found over the urban areas studied here and the corresponding mixture of positive and negative daytime LST anomalies. Further work is needed to understand this relationship for example through the application of atmospheric chemical transport models. Moreover, analysis of AAOD data demonstrated that all the selected cities (–0.1 to –2.65) and major parts of India (average –2.06) experienced a significant reduction of AAOD during the lockdown (Fig. S8). This reduction was mostly attributed to anthropogenic emissions associated with lockdown which can cause a decrease in atmospheric warming (Srivastava et al., 2021) as well as lower atmospheric temperature. It can be deduced that the observed variations in the net radiative flux are directly related to the lower emissions of aerosols due to human activities during the lockdown.

Air pollution is a major public health issue that caused premature deaths of 1.67 million in India in 2019 (Pandey et al., 2021), including 981,000 pre-term births in 2018 (Farrow et al., 2020). In urban and industrial regions of India, higher PM concentration has been associated with a reduction of life expectancy by 3.2 years for 660 million people in India (Cohen et al., 2017). Over the last five decades (1970–2020), clear air policies have been implemented by the Indian government to improve the standard of air quality. Pioneer emission control policies have been implemented by the Central Pollution Control Board (CPCB, 1974), National Ambient Air Quality Standards (NAAQS, 1994), MoEFCC action plan (1997), National Ambient Monitoring Programme (NAMP, 2016), and Graded Response Action Plan (GRAP, 2016) (Ganguly et al., 2020). The latest stringent emission control policies introduced are National Clean Air Program (NCAP, 2018), which aimed to reduce $PM_{2.5}$ pollution by 20–30% by 2024 in 122 non-attainment cities compared to 2017 levels. Under the NCAP, major action plans involve emission control from transport and road dust followed by interventions for the industrial and open waste burning. Emissions reduction policies are also supported by initiatives to promote green energy such as the National Action Plan on Climate Change (NAPCC, 2008) which aimed to promote the solar energy, electric vehicles, and the smart cities mission (Pandve, 2009) as abatement strategies towards mitigating air pollution. According to the "Vehicle Scrappage Policy 2021" guidelines, cars and commercial vehicles older than 20 and 15 years, respectively will be phased out for decreasing vehicular pollution by 25%.

During the initial lockdown period (i.e. 2 weeks in March) in India, it was estimated that about 5300 (1000–11700) premature deaths were averted due to reduced $PM_{2.5}$ concentrations (Venter et al., 2020). Whereas globally it was projected 0.78 (0.09–1.5) million premature deaths could be averted in 2020, assuming the lockdown scenarios throughout the year (Venter et al., 2020). In Europe and China, it is estimated that premature deaths were reduced by tens of thousands during the lockdown duration due to lower $PM_{2.5}$ concentrations and are projected to reduce by between 76,400 and 287,000 in China and by 13,600–29,500 in Europe if the lockdown scenario persisted through 2020 (Giani et al., 2020). Nevertheless, it is from the lockdown that an improvement in air quality was directly associated with a reduction in anthropogenic activity and illustrates the potential benefits that government clean air policies and green energy production could achieve in India. During the lockdown, the energy generation pattern shifted from non-renewal fuel to renewal by 6.5% (Parida et al., 2020). With the increasing use of renewable fuels and the shift towards green energy, India is contributing to climate change adaptation and mitigation policy. Reductions in $PM_{2.5}$ and NO_2 concentrations also suggest that future policies could target transport and industrial emissions. Whilst the focus of this study has been on the reduction in emissions and improvements to air quality due to the lockdown, the pandemic has also highlighted the need to update urban planning policies to make them more resilient and sustainable (e.g. Sustainable Development Goals, SDG-11) as highlighted by (Sharifi and Khavarian-Garmsir, 2020).

5. Conclusions

Satellite and surface atmospheric measurements across India during the first lockdown period (March–May 2020) revealed a widespread decrease in NO_2 (average of 12% in tropospheric) which was particularly apparent over the six cities that were the focus of this study (average decrease of 31.5% in tropospheric). Decreases in $PM_{2.5}$ concentration were also evident although more variable than that of NO_2 due to the wider range of potential emissions sources although, with the exception of Hyderabad, all cities recorded average decrease of AOD between 10 and 80%. The reduction in a significant proportion of these pollutants is most likely due to the confinement measures imposed to restrict the spread of the COVID-19, which subsequently resulted in the abrupt reduction in transport (i.e. surface and air traffic) and industrial activities. Over the same time period, MODIS day and night LST data indicate a decrease in temperature relative to the same period over the preceding 5 years over the northern and eastern parts of India. The MODIS LST and in-situ air temperature measurements indicate decreases and increases in temperature over the urban areas which don't all vary in relation to the anomalies in AOD (as a proxy for $PM_{2.5}$) highlighting the complex interaction between these variables. Whilst further research is needed to understand the linkages between air pollution and surface temperature, the reduction in population mobility during the lockdown has illustrated the potential gains that can be made with respect to air quality by reducing anthropogenic emissions, particularly those from transportation. Given that it is estimated that 68% of the world's population will reside in urban areas by 2050 (United Nations Department of Economic and Social Affairs, 2019), policies to improve to air quality and the design of urban environments are needed to help meet SDG-11 and to make urban areas more resilient.

Credit author statement

Bikash Ranjan Parida: Conceptualization, Investigation, Methodology, Software, Formal analysis, Writing & editing –original draft. Somnath Bar: Conceptualization, Investigation, Methodology, Software, Formal analysis, Writing & editing –original draft. Shyama Prasad Mandal: Conceptualization, Methodology, Software. Arvind Chandra Pandey: Conceptualization, Supervision, Data support, Writing – review & editing. Manoj Kumar: Conceptualization, Supervision, Data support, Writing – review & editing. Gareth Roberts: Conceptualization, Formal analysis, Writing – review & editing. Jadunandan Dash: Conceptualization, Formal analysis, Writing – review & editing.

Declaration of competing interest

The authors declare that they have no known competing financial interests or personal relationships that could have appeared to influence the work reported in this paper.

Acknowledgements

Authors thanks to European Union, Copernicus Services for providing access to satellite-based NO_2 data (Sentinel–5P TROPOMI), NASA LPDAAC for provision of the MODIS LST and AOD data, and Google Earth Engine (GEE) for providing the analyzing platform. The authors also thank various organizations for providing access to ground observation data on NO_2 and $PM_{2.5}$. B.R Parida received funding from University Grants Commission under the start-up Grant (F.4–5(209-

FRP)/2015/BSR).

Appendix A. Supplementary data

Supplementary data to this article can be found online at https://doi.org/10.1016/j.envres.2021.111280.

References

Abdullah, S., Mansor, A.A., Napi, N.N.L.M., Mansor, W.N.W., Ahmed, A.N., Ismail, M., Ramly, Z.T.A., 2020. Air quality status during 2020 Malaysia Movement Control Order (MCO) due to 2019 novel coronavirus (2019-nCoV) pandemic. Sci. Total Environ. 729, 139022. https://doi.org/10.1016/j.scitotenv.2020.139022.

Achakulwisut, P., Brauer, M., Hystad, P., Anenberg, S.C., 2019. Global, national, and urban burdens of paediatric asthma incidence attributable to ambient NO2 pollution: estimates from global datasets. Lancet Planet. Health 3, e166–e178. https://doi.org/10.1016/S2542-5196(19)30046-4.

Acharya, P., Barik, G., Gayen, B.K., Bar, S., Maiti, A., Sarkar, A., Ghosh, S., De, S.K., Sreekesh, S., 2021. Revisiting the levels of Aerosol Optical Depth in south-southeast Asia, Europe and USA amid the COVID-19 pandemic using satellite observations. Environ. Res. 193, 110514. https://doi.org/10.1016/j.envres.2020.110514.

Anenberg, S.C., Miller, J., Minjares, R., Du, L., Henze, D.K., Lacey, F., Malley, C.S., Emberson, L., Franco, V., Klimont, Z., Heyes, C., 2017. Impacts and mitigation of excess diesel-related NOx emissions in 11 major vehicle markets. Nature 545, 467–471. https://doi.org/10.1038/nature22086.

Balakrishnan, K., Dey, S., Gupta, T., Dhaliwal, R.S., Brauer, M., Cohen, A.J., et al., 2019. The impact of air pollution on deaths, disease burden, and life expectancy across the states of India: the Global Burden of Disease Study 2017. Lancet Planet. Health 3, e26–e39. https://doi.org/10.1016/S2542-5196(18)30261-4.

Barragan, R., Molero, F., Granados-Muñoz, M.J., Salvador, P., Pujadas, M., Artíñano, B., 2020. Feasibility of ceilometers data to estimate radiative forcing values: application to different conditions around the COVID-19 lockdown period. Rem. Sens. 12, 3699. https://doi.org/10.3390/rs12223699.

Bauwens, M., Compernolle, S., Stavrakou, T., Müller, J.-F., Gent, J., Eskes, H., Levelt, P. F., A, R., Veefkind, J.P., Vlietinck, J., Yu, H., Zehner, C., 2020. Impact of coronavirus outbreak on NO2 pollution assessed using TROPOMI and OMI observations. Geophys. Res. Lett. 47 https://doi.org/10.1029/2020GL087978.

Beirle, S., Platt, U., Wenig, M., Wagner, T., 2003. Weekly cycle of NO2 by GOME measurements: a signature of anthropogenic sources. Atmos. Chem. Phys. 3, 2225–2232. https://doi.org/10.5194/acp-3-2225-2003.

Bera, B., Bhattacharjee, S., Shit, P.K., Sengupta, N., Saha, S., 2020. Significant impacts of COVID-19 lockdown on urban air pollution in Kolkata (India) and amelioration of environmental health. Environ. Dev. Sustain. https://doi.org/10.1007/s10668-020-00898-5.

Biswal, A., Singh, T., Singh, V., Ravindra, K., Mor, S., 2020. COVID-19 lockdown and its impact on tropospheric NO2 concentrations over India using satellite-based data. Heliyon 6, e04764. https://doi.org/10.1016/j.heliyon.2020.e04764.

Boersma, K.F., Eskes, H.J., Brinksma, E.J., 2004. Error analysis for tropospheric NO2 retrieval from space. J. Geophys. Res. Atmospheres 109. https://doi.org/10.1029/2003JD003962.

Cede, A., Herman, J., Richter, A., Krotkov, N., Burrows, J., 2006. Measurements of nitrogen dioxide total column amounts using a Brewer double spectrophotometer in direct Sun mode. J. Geophys. Res. 111, D05304. https://doi.org/10.1029/2005JD006585.

Chauhan, A., Inskip, H.M., Linaker, C.H., Smith, S., Schreiber, J., Johnston, S.L., Holgate, S.T., 2003. Personal exposure to nitrogen dioxide (NO2) and the severity of virus-induced asthma in children. Lancet 361, 1939–1944. https://doi.org/10.1016/S0140-6736(03)13582-9.

Chauhan, A., Singh, R.P., 2020. Decline in PM2.5 concentrations over major cities around the world associated with COVID-19. Environ. Res. 187, 109634. https://doi.org/10.1016/j.envres.2020.109634.

Chen, Q.-X., Huang, C.-L., Yuan, Y., Tan, H.-P., 2020. Influence of COVID-19 event on air quality and their association in mainland China. Aerosol Air Qual. Res. 20, 1541–1551. https://doi.org/10.4209/aaqr.2020.05.0224.

Chen, R., Samoli, E., Wong, C.-M., Huang, W., Wang, Z., Chen, B., Kan, H., 2012. Associations between short-term exposure to nitrogen dioxide and mortality in 17 Chinese cities: the China Air Pollution and Health Effects Study (CAPES). Environ. Int. 45, 32–38. https://doi.org/10.1016/j.envint.2012.04.008.

Chu, L., Oloo, F., Bergstedt, H., Blaschke, T., 2020. Assessing the link between human modification and changes in land surface temperature in hainan, China using image archives from Google Earth engine. Rem. Sens. 12, 888. https://doi.org/10.3390/rs12050888.

Cohen, A.J., Brauer, M., Burnett, R., Anderson, H.R., Frostad, J., Estep, K., et al., 2017. Estimates and 25-year trends of the global burden of disease attributable to ambient air pollution: an analysis of data from the Global Burden of Diseases Study 2015. Lancet 389, 1907–1918. https://doi.org/10.1016/S0140-6736(17)30505-6.

Crippa, M., Guizzardi, D., Muntean, M., Schaaf, E., Dentener, F., van Aardenne, J.A., Monni, S., Doering, U., Olivier, J.G.J., Pagliari, V., Janssens-Maenhout, G., 2018. Gridded emissions of air pollutants for the period 1970–2012 within EDGAR v4.3.2. Earth Syst. Sci. Data 10, 1987–2013. https://doi.org/10.5194/essd-10-1987-2018.

CWOP, 2020. Citizen weather observer Program. Available online: http://www.wxqa.com. (Accessed 10 July 2020).

Dantas, G., Siciliano, B., França, B.B., da Silva, C.M., Arbilla, G., 2020. The impact of COVID-19 partial lockdown on the air quality of the city of Rio de Janeiro, Brazil. Sci. Total Environ. 729, 139085. https://doi.org/10.1016/j.scitotenv.2020.139085.

Dentener, F., Stevenson, D., Ellingsen, K., van Noije, T., Schultz, M., Amann, M., et al., 2006. The global atmospheric environment for the next generation. Environ. Sci. Technol. 40, 3586–3594. https://doi.org/10.1021/es0523845.

Dutheil, F., Baker, J.S., Navel, V., 2020. COVID-19 as a factor influencing air pollution? Environ. Pollut. 263, 114466. https://doi.org/10.1016/j.envpol.2020.114466.

Farrow, A., Miller, K.A., Myllyvirt, L., 2020. Toxic Air: the Price of Fossil Fuels. Greenpeace Southeast Asia, Seoul. Available online: https://www.greenpeace.org/static/planet4-southeastasia-stateless/2020/02/21b480fa-toxic-air-report-110220.pdf. (Accessed 28 January 2021).

Filonchyk, M., Hurynovich, V., Yan, H., Gusev, A., Shpilevskaya, N., 2020. Impact assessment of COVID-19 on variations of SO2, NO2, CO and AOD over East China. Aerosol Air Qual. Res. 20, 1530–1540. https://doi.org/10.4209/aaqr.2020.05.0226.

Ganguly, T., Selvaraj, K.L., Guttikunda, S.K., 2020. National Clean Air Programme (NCAP) for Indian cities: review and outlook of clean air action plans. Atmos. Environ. X 8, 100096. https://doi.org/10.1016/j.aeaoa.2020.100096.

Gautam, S., 2020. COVID-19: air pollution remains low as people stay at home. Air Qual. Atmosphere Health. https://doi.org/10.1007/s11869-020-00842-6.

Giani, P., Castruccio, S., Anav, A., Howard, D., Hu, W., Crippa, P., 2020. Short-term and long-term health impacts of air pollution reductions from COVID-19 lockdowns in China and Europe: a modelling study. Lancet Planet. Health 4, e474–e482. https://doi.org/10.1016/S2542-5196(20)30224-2.

Gogoi, P.P., Vinoj, V., Swain, D., Roberts, G., Dash, J., Tripathy, S., 2019. Land use and land cover change effect on surface temperature over Eastern India. Sci. Rep. 9, 8859. https://doi.org/10.1038/s41598-019-45213-z.

Goldberg, D.L., Anenberg, S.C., Griffin, D., McLinden, C.A., Lu, Z., Streets, D.G., 2020. Disentangling the impact of the COVID-19 lockdowns on urban NO_2 from natural variability. Geophys. Res. Lett. 47 https://doi.org/10.1029/2020GL089269.

Gorelick, N., Hancher, M., Dixon, M., Ilyushchenko, S., Thau, D., Moore, R., 2017. Google Earth engine: planetary-scale geospatial analysis for everyone. Remote Sens. Environ. 202, 18–27. https://doi.org/10.1016/j.rse.2017.06.031.

Griffin, D., Zhao, X., McLinden, C.A., Boersma, F., Bourassa, A., Dammers, E., et al., 2019. High-resolution mapping of nitrogen dioxide with TROPOMI: first results and validation over the Canadian oil sands. Geophys. Res. Lett. 46, 1049–1060. https://doi.org/10.1029/2018GL081095.

Gupta, A., Bhatt, C.M., Roy, A., Chauhan, P., 2020. COVID-19 lockdown a window of opportunity to understand the role of human activity on forest fire incidences in the Western Himalaya, India. Curr. Sci. 119, 390–397.

Ialongo, I., Virta, H., Eskes, H., Hovila, J., Douros, J., 2020. Comparison of TROPOMI/Sentinel-5 Precursor NO2 observations with ground-based measurements in Helsinki. Atmospheric Meas. Tech. 13, 205–218. https://doi.org/10.5194/amt-13-205-2020.

IEA, 2020. Changes in Transport Behaviour during the Covid-19 Crisis. IEA, Paris. https://www.iea.org/articles/changes-in-transport-behaviour-during-the-covid-19-crisis.

Jain, S., Sharma, T., 2020. Social and travel lockdown impact considering coronavirus disease (COVID-19) on air quality in megacities of India: present benefits, future challenges and way forward. Aerosol Air Qual. Res. 20, 1222–1236. https://doi.org/10.4209/aaqr.2020.04.0171.

JHU, 2021. New Cases of COVID-19 in World Countries. COVID-19 Dashboard by the Center for Systems Science and Engineering (CSSE) at Johns Hopkins University (JHU). Available online: https://coronavirus.jhu.edu/data/new-cases. (Accessed 12 February 2021).

Jin, M., Dickinson, R.E., Zhang, D., 2005. The footprint of urban areas on global climate as characterized by MODIS. J. Clim. 18, 1551–1565. https://doi.org/10.1175/JCLI3334.1.

Jin, M., Shepherd, J.M., Zheng, W., 2010. Urban surface temperature reduction via the urban aerosol direct effect: a remote sensing and wrf model sensitivity study. Adv. Meteorol. 2010, 1–14. https://doi.org/10.1155/2010/681587.

Kanniah, K.D., Kamarul Zaman, N.A.F., Kaskaoutis, D.G., Latif, M.T., 2020. COVID-19's impact on the atmospheric environment in the Southeast Asia region. Sci. Total Environ. 736, 139658. https://doi.org/10.1016/j.scitotenv.2020.139658.

Kaufman, Y.J., Koren, I., 2006. Smoke and pollution aerosol effect on cloud cover. Science 313, 655–658. https://doi.org/10.1126/science.1126232.

Kennedy, C.M., Oakleaf, J.R., Theobald, D.M., Baruch-Mordo, S., Kiesecker, J., 2019. Managing the middle: a shift in conservation priorities based on the global human modification gradient. Global Change Biol. 25, 811–826. https://doi.org/10.1111/gcb.14549.

Kim, M.J., 2019. Changes in the relationship between particulate matter and surface temperature in seoul from 2002–2017. Atmosphere 10, 238. https://doi.org/10.3390/atmos10050238.

Kratz, D.P., Stackhouse, P.W., Gupta, S.K., Wilber, A.C., Sawaengphokhai, P., McGarragh, G.R., 2014. The Fast longwave and shortwave flux (FLASHFlux) data product: single-scanner footprint fluxes. J. Appl. Meteorol. Climatol. 53, 1059–1079. https://doi.org/10.1175/JAMC-D-13-061.1.

Kumar, P., Hama, S., Omidvarborna, H., Sharma, A., Sahani, J., Abhijith, K.V., Debele, S. E., Zavala-Reyes, J.C., Barwise, Y., Tiwari, A., 2020. Temporary reduction in fine particulate matter due to 'anthropogenic emissions switch-off' during COVID-19 lockdown in Indian cities. Sustain. Cities Soc. 62, 102382. https://doi.org/10.1016/j.scs.2020.102382.

Kumar, S., 2020. Effect of meteorological parameters on spread of COVID-19 in India and air quality during lockdown. Sci. Total Environ. 745, 141021. https://doi.org/10.1016/j.scitotenv.2020.141021.

Lal, P., Kumar, A., Kumar, S., Kumari, S., Saikia, P., Dayanandan, A., Adhikari, D., Khan, M.L., 2020. The dark cloud with a silver lining: assessing the impact of the SARS COVID-19 pandemic on the global environment. Sci. Total Environ. 139297. https://doi.org/10.1016/j.scitotenv.2020.139297.

Larson, K., Hartmann, D.L., 2003. Interactions among cloud, water vapor, radiation, and large-scale circulation in the tropical climate. Part II: sensitivity to spatial gradients of sea surface temperature. J. Clim. 16, 1441–1455. https://doi.org/10.1175/1520-0442-16.10.1441.

Le Quéré, C., Jackson, R.B., Jones, M.W., Smith, A.J.P., Abernethy, S., Andrew, R.M., De-Gol, A.J., Willis, D.R., Shan, Y., Canadell, J.G., Friedlingstein, P., Creutzig, F., Peters, G.P., 2020. Temporary reduction in daily global CO2 emissions during the COVID-19 forced confinement. Nat. Clim. Change. https://doi.org/10.1038/s41558-020-0797-x.

Le, T., Wang, Y., Liu, L., Yang, J., Yung, Y.L., Li, G., Seinfeld, J.H., 2020. Unexpected air pollution with marked emission reductions during the COVID-19 outbreak in China. Science 369, 702–706. https://doi.org/10.1126/science.abb7431.

Li, H., Meier, F., Lee, X., Chakraborty, T., Liu, J., Schaap, M., Sodoudi, S., 2018. Interaction between urban heat island and urban pollution island during summer in Berlin. Sci. Total Environ. 636, 818–828. https://doi.org/10.1016/j.scitotenv.2018.04.254.

Li, L., Gu, X.-F., Yu, T., Hu, X.-Q., Chen, L.-F., Cheng, T.-H., 2009. Influence of dust aerosol on the brightness temperature of thermal infrared split window and land surface temperature retrieval. J. Infrared Millim. Waves 28, 102–106. https://doi.org/10.3724/SP.J.1010.2009.00102.

Lin, C., Li, Y., Yuan, Z., Lau, A.K.H., Li, C., Fung, J.C.H., 2015. Using satellite remote sensing data to estimate the high-resolution distribution of ground-level PM2.5. Remote Sens. Environ. 156, 117–128. https://doi.org/10.1016/j.rse.2014.09.015.

Liu, T., Marlier, M.E., DeFries, R.S., Westervelt, D.M., Xia, K.R., Fiore, A.M., Mickley, L.J., Cusworth, D.H., Milly, G., 2018. Seasonal impact of regional outdoor biomass burning on air pollution in three Indian cities: Delhi, Bengaluru, and Pune. Atmos. Environ. 172, 83–92. https://doi.org/10.1016/j.atmosenv.2017.10.024.

Liu, Z., Deng, Z., Ciais, P., Lei, R., Davis, S.J., Feng, S., Zheng, B., Cui, D., Dou, X., He, P., Zhu, B., Lu, C., Ke, P., Sun, T., Wang, Yuan, Yue, X., Wang, Yilong, Lei, Y., Zhou, H., Cai, Z., Wu, Y., Guo, R., Han, T., Xue, J., Boucher, O., Chevallier, F., Boucher, E., Wei, Y., Zhang, Q., Guan, D., Gong, P., Kammen, D.M., He, K., Schellnhuber, H.J., 2020. COVID-19 causes record decline in global CO2 emissions. ArXiv200413614 Phys. Q-Fin.

Loeb, N.G., Doelling, D.R., Wang, H., Su, W., Nguyen, C., Corbett, J.G., Liang, L., Mitrescu, C., Rose, F.G., Kato, S., 2018. Clouds and the Earth's radiant energy system (CERES) energy balanced and filled (EBAF) top-of-atmosphere (TOA) edition-4.0 data product. J. Clim. 31, 895–918. https://doi.org/10.1175/JCLI-D-17-0208.1.

Lyapustin, A.I., Wang, Y., Laszlo, I., Hilker, T., Hall, F.G., Sellers, P.J., Tucker, C.J., Korkin, S.V., 2012. Multi-angle implementation of atmospheric correction for MODIS (MAIAC): 3. Atmospheric correction. Remote Sens. Environ. 127, 385–393. https://doi.org/10.1016/j.rse.2012.09.002.

Mahato, S., Pal, S., Ghosh, K.G., 2020. Effect of lockdown amid COVID-19 pandemic on air quality of the megacity Delhi, India. Sci. Total Environ. 730, 139086. https://doi.org/10.1016/j.scitotenv.2020.139086.

McLinden, C.A., Fioletov, V., Boersma, K.F., Krotkov, N., Sioris, C.E., Veefkind, J.P., Yang, K., 2012. Air quality over the Canadian oil sands: a first assessment using satellite observations. Geophys. Res. Lett. 39 https://doi.org/10.1029/2011GL050273 n/a-n/a.

Mhawish, A., Banerjee, T., Sorek-Hamer, M., Lyapustin, A., Broday, D.M., Chatfield, R., 2019. Comparison and evaluation of MODIS multi-angle implementation of atmospheric correction (MAIAC) aerosol product over south Asia. Remote Sens. Environ. 224, 12–28. https://doi.org/10.1016/j.rse.2019.01.033.

Ming, Y., Lin, P., Naik, V., Paulot, F., Horowitz, L.W., Ginoux, P.A., Ramaswamy, V., Loeb, N.G., Shen, Z., Singer, C.E., Ward, R.X., Zhang, Z., Bellouin, N., 2021. Assessing the influence of COVID-19 on the shortwave radiative fluxes over the East asian marginal seas. Geophys. Res. Lett. 48 https://doi.org/10.1029/2020GL091699.

Muhammad, S., Long, X., Salman, M., 2020. COVID-19 pandemic and environmental pollution: a blessing in disguise? Sci. Total Environ. 728, 138820. https://doi.org/10.1016/j.scitotenv.2020.138820.

Munster, V.J., Koopmans, M., van Doremalen, N., van Riel, D., de Wit, E., 2020. A novel coronavirus emerging in China — key questions for impact assessment. N. Engl. J. Med. 382, 692–694. https://doi.org/10.1056/NEJMp2000929.

Nanda, D., Mishra, D.R., Swain, D., 2021. COVID-19 lockdowns induced land surface temperature variability in mega urban agglomerations in India. Environ. Sci. Process. Impacts 23, 144–159. https://doi.org/10.1039/D0EM00358A.

Navinya, C., Patidar, G., Phuleria, H.C., 2020. Examining effects of the COVID-19 national lockdown on ambient air quality across urban India. Aerosol Air Qual. Res. 20, 1759–1771. https://doi.org/10.4209/aaqr.2020.05.0256.

Pal, S.C., Chowdhuri, I., Saha, A., Chakrabortty, R., Roy, P., Ghosh, M., Shit, M., 2020. Improvement in ambient-air-quality reduced temperature during the COVID-19 lockdown period in India. Environ. Dev. Sustain. https://doi.org/10.1007/s10668-020-01034-z.

Pandey, A., Brauer, M., Cropper, M.L., Balakrishnan, K., Mathur, P., et al., 2021. Health and economic impact of air pollution in the states of India: the Global Burden of Disease Study 2019. Lancet Planet. Health 5, e25–e38. https://doi.org/10.1016/S2542-5196(20)30298-9.

Pandey, A.K., Singh, S., Berwal, S., Kumar, D., Pandey, P., Prakash, A., Lodhi, N., Maithani, S., Jain, V.K., Kumar, K., 2014. Spatio – temporal variations of urban heat island over Delhi. Urban Clim 10, 119–133. https://doi.org/10.1016/j.uclim.2014.10.005.

Pandve, H.T., 2009. India's national action plan on climate change. Indian J. Occup. Environ. Med. 13, 17. https://doi.org/10.4103/0019-5278.50718.

Pant, P., Lal, R.M., Guttikunda, S.K., Russell, A.G., Nagpure, A.S., Ramaswami, A., Peltier, R.E., 2019. Monitoring particulate matter in India: recent trends and future outlook. Air Qual. Atmosphere Health 12, 45–58. https://doi.org/10.1007/s11869-018-0629-6.

Papale, D., 2020. Clear evidence of reduction in urban CO2 emissions as a result of COVID-19 lockdown across Europe. Available online: http://www.icos-cp.eu/objects/w6pTmRGYKqAm3c-siQrg5kgd. accessed on: 9 September 2020.

Parida, B.R., Bar, S., Singh, N., Oinam, B., Pandey, A.C., Kumar, M., 2020. A short-term decline in anthropogenic emission of CO2 in India due to COVID-19 confinement. Prog. Phys. Geogr. 1–17. https://doi.org/10.1177/0309133320966741.

Qian, Y., Kaiser, D.P., Leung, L.R., Xu, M., 2006. More frequent cloud-free sky and less surface solar radiation in China from 1955 to 2000. Geophys. Res. Lett. 33, 1–4. https://doi.org/10.1029/2005GL024586.

Ranjan, A.K., Patra, A.K., Gorai, A.K., 2020. Effect of lockdown due to SARS COVID-19 on aerosol optical depth (AOD) over urban and mining regions in India. Sci. Total Environ. 745, 141024. https://doi.org/10.1016/j.scitotenv.2020.141024.

Rosenfeld, D., 2000. Suppression of rain and snow by urban and industrial air pollution. Science 287, 1793–1796. https://doi.org/10.1126/science.287.5459.1793.

Roy, S.S., 2008. Impact of aerosol optical depth on seasonal temperatures in India: a spatio-temporal analysis. Int. J. Rem. Sens. 29, 727–740. https://doi.org/10.1080/01431160701352121.

Safarian, S., Unnthorsson, R., Richter, C., 2020. Effect of coronavirus disease 2019 on CO2 emission in the world. Aerosol Air Qual. Res. 20, 1197–1203. https://doi.org/10.4209/aaqr.2020.04.0151.

Sahani, N., Goswami, S.K., Saha, A., 2020. The impact of COVID-19 induced lockdown on the changes of air quality and land surface temperature in Kolkata city, India. Spat. Inf. Res. https://doi.org/10.1007/s41324-020-00372-4.

SEDAC, 2020. Socioeconomic Data and Applications Center (Sedac). A Data Center in NASA's Earth Observing System Data and Information System (EOSDIS)- Hosted by CIESIN at Columbia University. Available online: https://sedac.ciesin.columbia.edu/data/collection/gpw-v4.

Sharifi, A., Khavarian-Garmsir, A.R., 2020. The COVID-19 pandemic: impacts on cities and major lessons for urban planning, design, and management. Sci. Total Environ. 749, 142391. https://doi.org/10.1016/j.scitotenv.2020.142391.

Sharma, S., Zhang, M., Anshika, Gao, J., Zhang, H., Kota, S.H., 2020. Effect of restricted emissions during COVID-19 on air quality in India. Sci. Total Environ. 728, 138878. https://doi.org/10.1016/j.scitotenv.2020.138878.

Shrestha, A.M., Shrestha, U.B., Sharma, R., Bhattarai, S., Tran, H.N.T., Rupakheti, M., 2020. Lockdown caused by COVID-19 pandemic reduces air pollution in cities worldwide (preprint). Down Earth. https://doi.org/10.31223/osf.io/edt4j.

Siciliano, B., Carvalho, G., da Silva, C.M., Arbilla, G., 2020. The impact of COVID-19 partial lockdown on primary pollutant concentrations in the atmosphere of rio de Janeiro and são paulo megacities (Brazil). Bull. Environ. Contam. Toxicol. 105, 2–8. https://doi.org/10.1007/s00128-020-02907-9.

Siddiqui, A., Halder, S., Chauhan, P., Kumar, P., 2020. COVID-19 pandemic and city-level nitrogen dioxide (NO2) reduction for urban centres of India. J. Indian Soc. Remote Sens. https://doi.org/10.1007/s12524-020-01130-7.

Singh, V., Singh, S., Biswal, A., Kesarkar, A.P., Mor, S., Ravindra, K., 2020. Diurnal and temporal changes in air pollution during COVID-19 strict lockdown over different regions of India. Environ. Pollut. 266, 115368. https://doi.org/10.1016/j.envpol.2020.115368.

Song, Z., Li, R., Qiu, R., Liu, S., Tan, C., Li, Q., Ge, W., Han, X., Tang, X., Shi, W., Song, L., Yu, W., Yang, H., Ma, M., 2018. Global land surface temperature influenced by vegetation cover and PM2.5 from 2001 to 2016. Rem. Sens. 10, 2034. https://doi.org/10.3390/rs10122034.

Srivastava, A.K., Bhoyar, P.D., Kanawade, V.P., Devara, P.C.S., Thomas, A., Soni, V.K., 2021. Improved air quality during COVID-19 at an urban megacity over the Indo-Gangetic Basin: from stringent to relaxed lockdown phases. Urban Clim 36, 100791. https://doi.org/10.1016/j.uclim.2021.100791.

Sun, C., Luo, Y., Li, J., 2018. Urban traffic infrastructure investment and air pollution: evidence from the 83 cities in China. J. Clean. Prod. 172, 488–496. https://doi.org/10.1016/j.jclepro.2017.10.194.

Theobald, D.M., Kennedy, C., Chen, B., Oakleaf, J., Baruch-Mordo, S., Kiesecker, J., 2020. Earth transformed: detailed mapping of global human modification from 1990 to2017 (preprint). Antroposhere - Land Cover and Land Use. https://doi.org/10.5194/essd-2019-252.

Tibbetts, J.H., 2015. Air quality and climate change: a delicate balance. Environ. Health Perspect. 123 https://doi.org/10.1289/ehp.123-A148.

Tobías, A., Carnerero, C., Reche, C., Massagué, J., Via, M., Minguillón, M.C., Alastuey, A., Querol, X., 2020. Changes in air quality during the lockdown in Barcelona (Spain) one month into the SARS-CoV-2 epidemic. Sci. Total Environ. 726, 138540. https://doi.org/10.1016/j.scitotenv.2020.138540.

Torres, O., Bhartia, P.K., Jethva, H., Ahn, C., 2018. Impact of the ozone monitoring instrument row anomaly on the long-term record of aerosol products. Atmospheric Meas. Tech. 11, 2701–2715. https://doi.org/10.5194/amt-11-2701-2018.

United Nations Department of Economic and Social Affairs, 2019. World population prospects 2019. Available online: https://population.un.org/wpp/. (Accessed 11 February 2021).

Vadrevu, K.P., Eaturu, A., Biswas, S., Lasko, K., Sahu, S., Garg, J.K., Justice, C., 2020. Spatial and temporal variations of air pollution over 41 cities of India during the COVID-19 lockdown period. Sci. Rep. 10, 16574. https://doi.org/10.1038/s41598-020-72271-5.

Veefkind, J.P., Aben, I., McMullan, K., Förster, H., de Vries, J., et al., 2012. TROPOMI on the ESA Sentinel-5 Precursor: a GMES mission for global observations of the

atmospheric composition for climate, air quality and ozone layer applications. Remote Sens. Environ. 120, 70–83. https://doi.org/10.1016/j.rse.2011.09.027.
Venter, Z.S., Aunan, K., Chowdhury, S., Lelieveld, J., 2020. COVID-19 lockdowns cause global air pollution declines with implications for public health risk (preprint). Epidemiology. https://doi.org/10.1101/2020.04.10.20060673.
Wan, Z., 2014. New refinements and validation of the collection-6 MODIS land-surface temperature/emissivity product. Remote Sens. Environ. 140, 36–45. https://doi.org/10.1016/j.rse.2013.08.027.
Wan, Z., 2008. New refinements and validation of the MODIS Land-Surface Temperature/Emissivity products. Remote Sens. Environ. 112, 59–74. https://doi.org/10.1016/j.rse.2006.06.026.
Wan, Z., Dozier, J., 1996. A generalized split-window algorithm for retrieving land-surface temperature from space. IEEE Trans. Geosci. Rem. Sens. 34, 892–905. https://doi.org/10.1109/36.508406.
Wang, D., Hu, B., Hu, C., Zhu, F., Liu, X., Zhang, J., Wang, B., Xiang, H., Cheng, Z., Xiong, Y., Zhao, Y., Li, Y., Wang, X., Peng, Z., 2020. Clinical characteristics of 138 hospitalized patients with 2019 novel coronavirus–infected pneumonia in wuhan, China. J. Am. Med. Assoc. 323, 1061. https://doi.org/10.1001/jama.2020.1585.
Wang, Su, 2020. A preliminary assessment of the impact of COVID-19 on environment – a case study of China. Sci. Total Environ. 728, 138915. https://doi.org/10.1016/j.scitotenv.2020.138915.
Weather Underground, 2020. Weather Underground managed by IBM cloud. Available online: https://www.wunderground.com. (Accessed 2 June 2020).
Westervelt, D.M., Mascioli, N.R., Fiore, A.M., Conley, A.J., Lamarque, J.-F., Shindell, D. T., Faluvegi, G., Previdi, M., Correa, G., Horowitz, L.W., 2020. Local and remote mean and extreme temperature response to regional aerosol emissions reductions. Atmos. Chem. Phys. 20, 3009–3027. https://doi.org/10.5194/acp-20-3009-2020.
WHO, 2020. Listings of WHO's response to COVID-19. https://www.who.int/news/item/29-06-2020-covidtimeline. (Accessed 26 January 2021).
WHO, 2016. WHO Ambient (outdoor) air pollution. Available online: https://www.who.int/en/news-room/fact-sheets/detail/ambient-(outdoor)-air-quality-and-health. (Accessed 31 July 2020).
WHO, 2005. WHO Air quality guidelines for particulate matter, ozone, nitrogen dioxide and sulfur dioxide. Available online: https://www.who.int/airpollution/publications/aqg2005/en/.
Xing, Y., Xu, Y., Shi, M., Lian, Y., 2016. The impact of PM2.5 on the human respiratory system. J. Thorac. Dis. 8, E69–E74 https://dx.doi.org/10.3978%2Fj.issn.2072-1439.2016.01.19.
Yang, X., Zhao, C., Zhou, L., Wang, Y., Liu, X., 2016. Distinct impact of different types of aerosols on surface solar radiation in China: variation of Aerosol Radiative Effect. J. Geophys. Res. Atmospheres 121, 6459–6471. https://doi.org/10.1002/2016JD024938.
Zara, M., Boersma, K.F., De Smedt, I., Richter, A., Peters, E., van Geffen, J.H.G.M., Beirle, S., Wagner, T., Van Roozendael, M., Marchenko, S., Lamsal, L.N., Eskes, H.J., 2018. Improved slant column density retrieval of nitrogen dioxide and formaldehyde for OMI and GOME-2A from QA4ECV: intercomparison, uncertainty characterisation, and trends. Atmospheric Meas. Tech. 11, 4033–4058. https://doi.org/10.5194/amt-11-4033-2018.
Zhang, R., Zhang, Y., Lin, H., Feng, X., Fu, T.-M., Wang, Y., 2020. NOx emission reduction and recovery during COVID-19 in east China. Atmosphere 11, 433. https://doi.org/10.3390/atmos11040433.
Zheng, Yang, Wu, Marinello, 2019. Spatial variation of NO2 and its impact factors in China: an application of sentinel-5P products. Rem. Sens. 11, 1939. https://doi.org/10.3390/rs11161939.